2025, Scienceline Publication
World's Veterinary Journal
World Vet J, 15(4): 1120-1129.
ISSN 2322-4568

DOI: https://dx.doi.org/10.54203/scil.2025.wvj115
PII: S232245682500115-15

In Silico Study on Structure Prediction of Apical Membrane Antigen 1 in *Eimeria tenella*

Pham Hoang Son Hung[1]*, Ho Thi Dung[1], Duong Thanh Hai[1], and Tran Nguyen Thao[1]

Faculty of Animal Science and Veterinary Medicine, University of Agriculture and Forestry, Hue University, Hue city, 49000, Vietnam

*Corresponding author's Email: phamhoangsonhung@hueuni.edu.vn

SHORT COMMUTATION
Received: September 29, 2025
Revised: October 27, 2025
Accepted: November 30, 2025
Published: December 31, 2025

ABSTRACT

The micronemal apical membrane antigen 1 (AMA1) has been demonstrated to be critical for host cell invasion by apicomplexan parasites. The present study predicted the structure of *Eimeria tenella* AMA1 (EtAMA1) using AlphaFold3. The structural model ranked first by AlphaFold3 was selected for analysis after removing unreliable regions. Comparative structural analyses were performed between the resulting EtAMA1 model and the well-characterized *Plasmodium falciparum* AMA1 (PfAMA1) using PyMOL. The results indicated that domains I and II of EtAMA1 may adopt the PAN motif (a conserved structural fold consisting of a five-stranded β-sheet and an α-helix) stabilized by five disulfide bonds, similar to PfAMA1. In addition, aromatic residues within the ligand binding pocket of PfAMA1 are conserved in EtAMA1, except for the critical Y251. The Proline-rich DII loop at the corner of the conserved hydrophobic pocket in EtAMA1 is shorter than that of PfAMA1, which possibly makes the hydrophobic pocket wider. Notably, domain III of *Et*AMA1 is predicted to form a three-stranded β-sheet with no disordered loop and α-helix, which is different from *Plasmodium* AMA1 structures. The present study provided preliminary information on structural divergences of EtAMA1, based on AlphaFold3 prediction, underscoring the need for experimental validation and investigation of possible implications for the parasite invasion mechanism.

Keywords: Apical membrane antigen 1, Domain, Hydrophobic pocket, *Eimeria tenella*

INTRODUCTION

Coccidiosis, caused by the apicomplexan parasites of the genus *Eimeria*, is a common and devastating disease in the poultry industry, especially in broiler production (Blake et al., 2020). Seven pathogenic *Eimeria* species in chickens, including *Eimeria acervuline (E. acervuline), E. brunetti, E. praecox, E. mitis, E. necatrix, E. maxima,* and *E. tenella*, invade and damage specific sites in the chicken's gastrointestinal tract (Mathis et al., 2025). For example, *E. tenella* infects the ceca, while *E. maxima* invades the small intestine. Clinical symptoms of coccidiosis include diarrhea, reduced weight gain, and reduced feed conversion (Quiroz-Castaneda, 2018). Severe intestinal lesions leading to hemorrhagic necrosis may occur, ultimately resulting in mortality (Pham et al., 2021).

Eimeria parasites are placed within the phylum *Apicomplexa* with the human malaria parasite Plasmodium and other well-known parasites, including *Toxoplasma*, *Babesia*, *Cryptosporidium*, and *Theileria*. Despite their diverse hosts and life cycles, apicomplexan parasites employ a broadly conserved mechanism to invade host cells. Central to the invasion process is the formation of a moving junction (MJ) that requires the apical membrane antigen 1 (AMA1), which is secreted by micronemes and translocated to the parasite apical surface, to interact with the rhoptry neck protein 2 (RON2), which is secreted by rhoptries and inserted into the host cell membrane (Besteiro et al., 2009; 2011; Lamarque et al., 2011; Srinivasan et al., 2011; Tonkin et al., 2011; Harvey et al., 2014). The direct interaction between AMA1 and RON2 were first confirmed in *Toxoplasma gondii* (Besteiro et al., 2009) and later in *Plasmodium falciparum* (Srinivasan et al., 2011; Lamarque et al., 2011; Tonkin et al., 2011). AMA1 is a type I integral membrane protein, comprising a disordered N-terminal tail, the ectodomain (or extracellular domain), a single-helix transmembrane domain, and finally a C-terminal cytosolic tail. The ectodomain, composed of domain I (DI), domain II (DII), and domain III (DIII), forms the core and most essential structural element of AMA1. On the ectodomain of AMA1, the key binding site of RON2 is located at the hydrophobic pocket defined by residues at the apical surface of DI and a loop from DII (denoted as DII loop; Besteiro et al., 2011; Srinivasan et al., 2011; Tonkin et al., 2011). The base of this hydrophobic pocket contains hydrophobic residues that are conserved across various apicomplexan parasites, while polymorphic residues are located at the margin of the pocket (Bai et al., 2005). Based on its role in host cell invasion, AMA1 has been extensively studied as a potential vaccine candidate against the life-threatening malaria disease. Early clinical trials indicated that immunization with heterogenous AMA1 elicited protective immunity against *Plasmodium falciparum* (Chuang et al., 2013). Antibodies targeted DIII of PfAMA1 have been shown to impair erythrocyte penetration of merozoite

To cite this paper: Hung PHS, Dung HT, Hai DT, and Thao TN (2025). *In Silico* Study on Structure Prediction of Apical Membrane Antigen 1 in *Eimeria tenella. World Vet. J.*, 15(4): 1120-1129. DOI: https://dx.doi.org/10.54203/scil.2025.wvj115

Plasmodium falciparum, demonstrating that DIII contributes to functional epitopes that can be targeted to generate vaccines (Nair et al., 2002). However, the high polymorphism of PfAMA1 reduces its effectiveness as a vaccine (Ouattara et al., 2012). For *Eimeria* parasites that cause coccidiosis in birds, host cell invasion may also require the formation of the AMA1-RON2 complex, which is essential for the host cell invasion, analogous to what is found in *Plasmodium* (Wang et al., 2020). A study revealed that *Eimeria tenella* apical membrane antigen 1 (EtAMA1) is predominantly expressed at the sporozoite stage, during which the parasites invade the chick cecum's epithelial cells (Li et al., 2018). The recombinant *E. maxima* AMA1 (EmAMA1) expressed in *E. tenella*, when used as a vaccine component against *E. maxima*, provided partial protection against coccidiosis in chickens (Pastor-Fernandez et al., 2018). Similarly, inoculation of transgenic Lactic bacteria expressing EtAMA1 induced adaptive immune response (Liu et al., 2020) and mitigated oocyst shedding and cecal lesion severity in chicks challenged with homologous *E. tenella* (Li et al., 2018).

Despite the relevance of *Eimeria* AMA1 as a vaccine target for coccidiosis, the three-dimensional structure of AMA1 from *Eimeria* has not yet been experimentally determined. A search on the Protein Data Bank (PDB) identified no structural entries for *Eimeria* AMA1, confirming a significant gap in current knowledge and underscoring the need for structural prediction and comparative analysis of EtAMA1. In the present study, the 3D structure of *Eimeria tenella* apical membrane antigen 1 (EtAMA1) was predicted by AlphaFold3 and compared with previously characterized *Plasmodium* AMA1 structures to identify possible conserved and divergent features.

MATERIALS AND METHODS

Protein sequences

Protein sequences used for the multiple sequence alignment and structure prediction in the present study were retrieved from NCBI (Table 1).

Table 1. Protein sequences of apical membrane antigen 1 from *Plasmodium faciparum*, and different *Eimeria* species used for the sequence alignment

Protein	Species	NCBI accession number	Sequence length (amino acids)
PfAMA1	*Plasmodium falciparum*	UIH11214.1	622
EtAMA1	*Eimeria tenella*	AEJ33058.1	536
EmAMA1	*Eimeria maxima*	SNT95431.1	539
EiAMA1	*Eimeria intestinalis*	WIW69503.1	549
EbAMA1	*Eimeria brunetti*	BAM16294.1	551

Sequence alignment

Multiple sequence alignment was carried out using Clustal W in MEGAX 10.2.6 with gap-open penalties set to 10 and gap-extension penalties set to 0.2. Results were visualized using ESPript 3 (Robert and Gouet, 2014). The identical percentage was calculated by pairwise alignment between two sequences using MEGAX 10.2.6 with gap-open penalties set to 10 and gap-extension penalties set to 0.2.

Protein structure prediction

The full-length amino acid sequence of EtAMA1 (536 amino acids) was used for structural prediction with AlphaFold3 (AF3) under default settings (Abramson et al., 2024). AF3 outputted five structural models, which were ranked by the ranking _score, which incorporated the predicted template modeling (pTM) to reflect the global reliability of the predicted structure, a penalty for steric clashes, and a small gain for predicted disorder (Jumper et al., 2021; Abramson et al., 2024). The model ranked first by AF3 was chosen for subsequent analysis in this study. The local quality of the selected model was further justified considering the predicted local difference distance test (plDDT). The plDDT metric indicates the accuracy of predicted atomic position, using a 1-100 scale in which higher values indicate greater confidence of protein folding (Mariani et al., 2013; Guo et al., 2022; Abramson et al., 2024).

Structure visualization and analysis

The AF3-predicted structure of EtAMA1 was visualized and superimposed with the crystal structures of PfAMA1 (PDB ID: 1Z40) and *Plasmodium vivax* AMA1 (PvAMA1; PDB ID: 1W8K) using PyMOL (version 2.6, Schrodinger Inc). Root mean square deviation of atomic position (RMSD) values was calculated with the *super* command in PyMOL (Fukutani et al., 2021). As the crystal structure of PfAMA1 represents only residues 108-438, rather than the full-length PfAMA1 protein sequence, the RMSD calculation was performed by superimposing the PfAMA1 crystal structure with the corresponding region in EtAMA1 (residues 60-392). Specifically, five cycles of pairwise alignment and structural superposition between the Cα atoms of EtAMA1 and PfAMA1 were performed by PyMOL, during which outlier atoms (with RMSD > 2 Å) were rejected to eliminate poorly aligned regions. After rejection, the remaining 198 Cα atoms from each structure were superimposed.

RESULTS AND DISCUSSION

Sequence conservation among apical membrane antigen 1 proteins

Multiple sequence alignment of five AMA1 protein sequences from *Eimeria* and *Plasmodium* species revealed a relatively low conservation, with only 82 residues strictly conserved across all sequences (Figure 1). Among the strictly conserved residues, ten cysteine residues that form five disulfide bonds in domains I and II of PfAMA1 are also completely conserved in *Eimeria* AMA1 proteins, suggesting the conservation of these five disulfide linkages in AMA1 structure across two different genera. Protein sequences at the N-terminal region are highly variable between *Plasmodium falciparum* AMA1 (PfAMA1) and *Eimeria* AMA1, and among *Eimeria* AMA1 proteins. In addition, over 150 amino acids near the C-terminal end of PfAMA1 are not conserved in *Eimeria*, although the C-terminal end is highly conserved among the four *Eimeria* AMA1 proteins. The strictly conserved residues mainly locate in the central part of *Eimeria* AMA1, aligned with residues at the well-structured domain I and domain II of PfAMA1. Similar observations have been reported in AMA1 studies of parasites, where structural constraints preserve the fold despite extensive antigenic polymorphism (Bai et al., 2005).

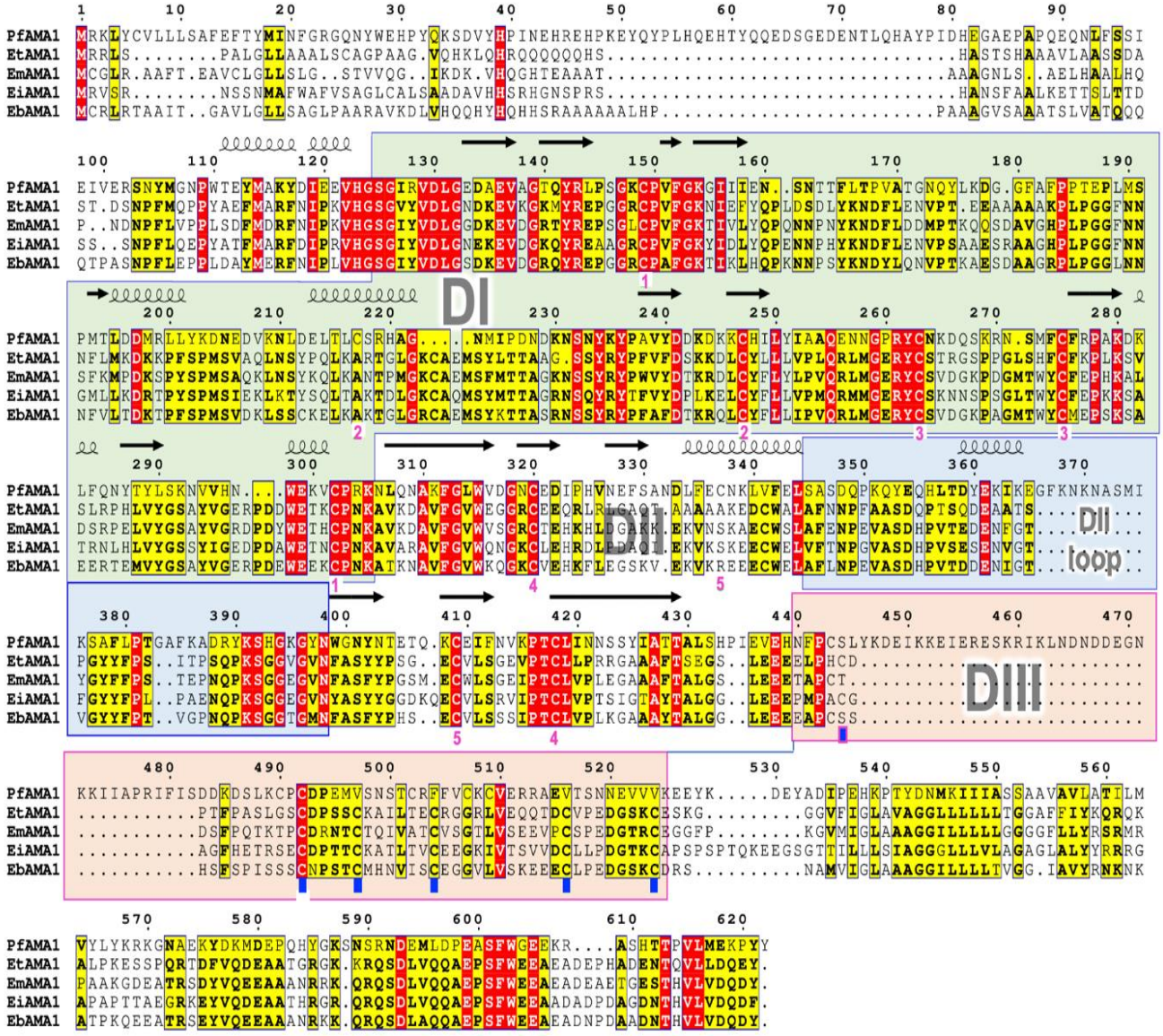

Figure 1. Multiple protein sequence alignment of apical membrane antigen 1 (AMA1) showing relationships between *Eimeria tenella* and *Plasmodium falciparum*. Helices and arrows above the alignment, respectively, represent α-helices and β-strands in the crystal structure of *P. falciparum AMA1* (PfAMA1). Pink numbers below mark cysteine residues forming disulfide bonds in PfAMA1. Blue squares indicate cysteine residues that are predicted to form disulfide bonds in domain III of *E. tenella* AMA1 (EtAMA1). Red shading marks strictly conserved residues; Yellow indicates residues conserved in most sequences. Domains I, II, and III, labelled respectively as DI, DII, and DIII, are marked with light green, transparent, and light peach backgrounds. The loop within Domain II participating in the hydrophobic pocket, labeled as DII loop, is marked with a light blue background.

Structural features of *Eimeria tenella* apical membrane antigen 1

First, the local quality of the AF3-predicted structure of EtAMA1 was assessed by plDDT scores (Figure 2A). Low plDDT scores (plDDT < 70) were observed in the N-terminal segment (residues 1-59), which likely corresponds to the disordered N-terminal tail, and the C-terminal segment (residues 441-536), which may include the transmembrane helix and the C-terminal cytosolic tail. As a low plDDT score indicates intrinsic disorder or structural uncertainty (Guo et al., 2022; Kovalevskiy et al., 2024), the two segments (1-59 and 441-536) were excluded from further structural analysis. The truncated AF3-predicted EtAMA1 model is predominantly high in pLDDT scores (> 90), indicating reliable folding predictions. The EtAMA1 structure was divided into four parts, including an N-terminal α-helix and three domains, denoted as domains I (DI), domain II (DII), and domain III (DIII; Figure 2B). Boundaries for the N-terminal α-helix, DI, and DII were inferred from the sequence alignment in Figure 1, using the domain boundaries defined in the crystal structure of PfAMA1 as a reference. DI and DII in the EtAMA1 model are packed against each other, consistent with the core structure of AMA1 ectodomain from *Plasmodium* and *Toxoplasma* (Bai et al., 2005; Crawford et al., 2010), suggesting that the overall architecture of AMA1 ectodomain may still have been preserved across the phylum despite low sequence identity. Detailed structural comparisons and discussions for each domain were presented in later sections.

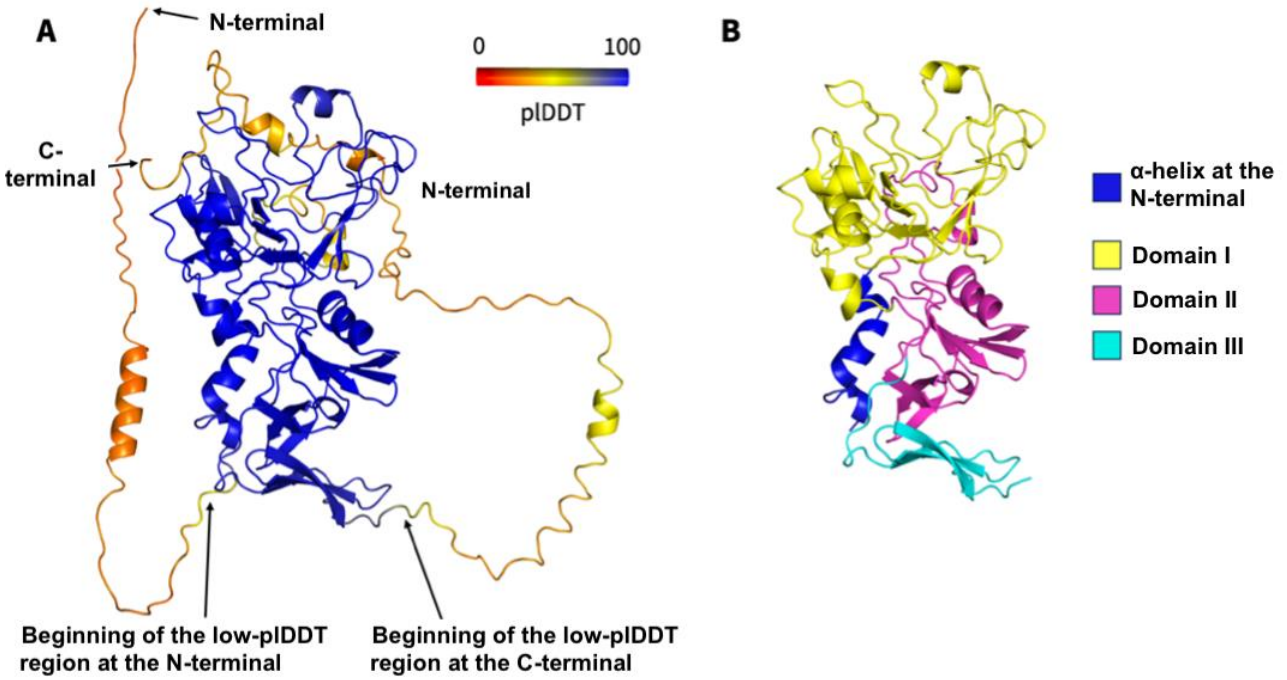

Figure 2. Predicted structure of *Eimeria tenella* apical membrane antigen 1 (EtAMA1) by AlphaFold. **A:** The AlphaFold3-predicted structure of EtAMA1 is colored according to the predicted local distance difference test (pLDDT) score, ranging from red (low confidence, pLDDT = 0) to blue (high confidence, pLDDT = 100). **B:** The AlphaFold3-predicted structure of EtAMA1 was trimmed to remove the N-terminal and C-terminal regions with low pLDDT scores. The final trimmed structure was colored by domain, with the N-terminal helix depicted in blue, domain I in yellow, domain II in pink, and domain III in cyan.

Conservation of the PAN motif in domains I and II

The N-terminal α-helix, DI and DII of EtAMA1 are predicted to closely resemble the corresponding domains in the crystallographic structure of PfAMA1 (PDB ID: 1Z40). The root mean square deviation between the crystal structure of PfAMA1 and the AF3-predicted structure of EtAMA1 (DIII and low plDDT-scoring regions excluded) was calculated to be 0.759 Å over 198 Cα atoms (aligned by PyMOL), suggesting high structural similarity, particularly in the core of DI and DII. Despite only 19% amino acid identity between EtAMA1 and PfAMA1, the folding characteristics of DI and DII may be conserved. DI and DII of EtAMA1 exhibited the classical PAN motif (Figure 3), a conserved structural fold consisting of a five-stranded β-sheet and an α-helix, found in DI and DII of PfAMA1 and *Toxoplasma gondii* AMA1 (TgAMA1; Bai et al., 2005; Pizarro et al., 2005; Crawford et al., 2010). Earlier reports in *Plasmodium* AMA1 indicated that disulfide bonds played a crucial role in maintaining the structural integrity of the AMA1 ectodomain (Bai et al., 2005). Similarly, ten cysteine residues were predicted to form five disulfide bonds in EtAMA1, all conserved across *Eimeria* species, possibly reinforcing the stability of DI and DII. Eight out of the ten cysteines are invariant compared to PfAMA1, while the remaining two cysteines are present but shifted by several residues relative to their positions in PfAMA1. The similarity in structural scaffold and cysteine framework between the EtAMA1 model and PfAMA1, inferred from AF3 prediction, suggested the possibility that EtAMA1 may engage in a function analogous to PfAMA1. Moreover, a low sequence identity between EtAMA1 and PfAMA1, in contrast to the anticipated preservation of their core folding within DI and DII, may suggest an evolutionary strategy that maintains essential functional architecture of DI and DII while allowing substantial polymorphism.

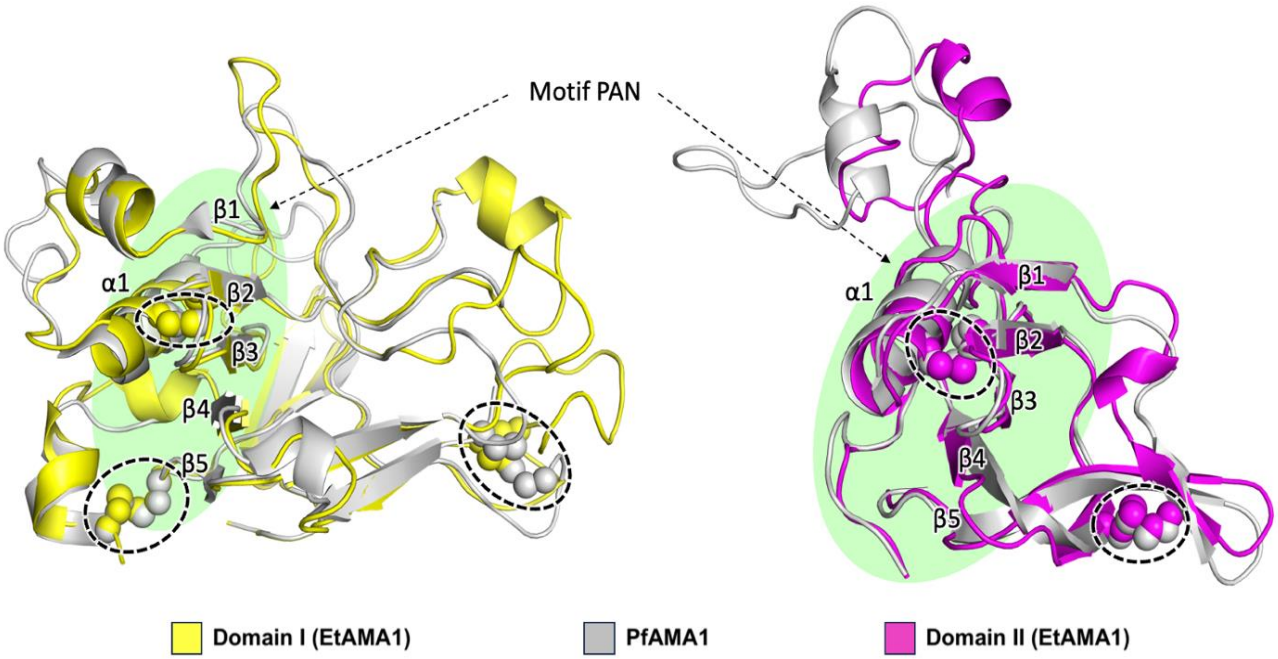

Figure 3. Structural comparison between domain I (left) and domain II (right) of *Eimeria tenella* apical membrane antigen 1 (EtAMA1) with that of *Plasmodium falciparum* apical membrane antigen 1 (PfAMA1). DI or DII of EtAMA1 and PfAMA1 were superimposed by PyMOL. Domain I and II of EtAMA1 are shown respectively in yellow and magenta, and the two domains in PfAMA1 are both colored in grey. Cysteine residues forming disulfides are shown as spheres, and the disulfide bridges are circled with dashed lines. The PAN motif, consisting of one α-helix (α1) and five β-strands (β1-β5), in each structure is highlighted with a light green-filled shape.

Variations of the critical residues from domain I at the conserved hydrophobic pocket for ligand binding

The binding partner of *Eimeria* AMA1 has not yet been identified; however, it is possible that *Eimeria* AMA1 also interacts with a RON2 orthologue, similar to the *Plasmodium* model. Superimposition of the EtAMA1 model into the PfAMA1 crystal structure (PDB ID: 1Z40) revealed that residues F181, Y234, Y236, F281, and F367 at the critical hydrophobic pocket of PfAMA1 for RON2 binding are also found in the AF3-predicted EtAMA1 model, respectively, as F149, Y198, Y200, F239, and F339. Interestingly, Y251 and I252 at the conserved hydrophobic pocket in PfAMA1 are replaced by L215 and V216 in EtAMA1 (Figure 4). Notably, Y251 in PfAMA1 has been recognized as a key residue mediating AMA1-RON2 interaction, and is conserved across AMA1 proteins from species of different genera, including *Plasmodium vivax*, *P. vivax*, *Toxoplasma gondii*, *Babesia bovis*, and *Neospora caninum* (Crawford et al., 2010). A study indicated that a single mutation at Y251 of PfAMA1 resulted in the loss of RON2-binding capacity, highlighting the critical role of this Tyrosine in determining ligand binding affinity (Srinivasan et al., 2011). It is not known why AMA1 in *Eimeria tenella*, *E. intestinalis*, and *E. brunetti*, except *E. maxima*, have a Leucine (L214 in EtAMA1) instead of a Tyrosine as Y251 in PfMATE in its otherwise conserved hydrophobic pocket. Substituting the amphipathic, aromatic Tyrosine residue with the smaller, hydrophobic yet non-aromatic Leucine residue may alter the interactions at the binding site. However, it should be noted that the structure predicted by AlphaFold3 is highly speculative and unverified by experimental data.

Divergence of the domain II loop between *Eimeria tenella* apical membrane antigen 1 and *Plasmodium falciparum* apical membrane antigen 1

Apart from the differences in critical residues from DI at the hydrophobic pocket, there are also differences in the DII loop. From the alignment in the present study, the sequences of the DII loop among *Eimeria* species are mainly well conserved, while they are significantly different from PfAMA1 (Figure 1). In addition, the DII loop in EtAMA1 is 12 residues shorter than that of PfAMA1. Although the majority of the DII loop from EtAMA1 is predicted to have no well-defined secondary structure (Figure 4), there are six Proline residues in the sequence of the DII loop, which could impose certain conformational constraints on the loop (Figure 1). Four out of six Prolines are completely conserved across *Eimeria*, while the number of Proline residues in the entire DII loop of PfAMA1 is only one. While the DII loop of PfAMA1 reaches Y251 on the base of the hydrophobic pocket, the DII loop of EtAMA1 in the predicted structure does not extend over the hydrophobic pocket and remains spatially distant from the Y251 equivalent (L214), seemingly providing more access to the hydrophobic pocket in EtAMA1 compared with PfAMA1 (PDB ID: 1Z40). The

hydrophobic pocket in EtAMA1 appears wider than that in PfAMA1, with the maximum width estimated (PyMOL) at about 17.4 Å for EtAMA1 and 11.1 Å for PfAMA1. Previously, the DII loop has been described as a gatekeeper, shielding the hydrophobic pocket in PfAMA1 and TgAMA1, before being lifted away to allow the formation of the AMA1-RON2 complex (Tonkin et al., 2011; Vulliez-Le Normand et al., 2012). In addition, DII loops also modulate ligand binding affinity, as genetically modifying the DII loop in PfAMA1 to shorten its length significantly hampered the ability of PfAMA1 to bind the cognate RON2 (Delgadillo et al., 2016). The DII loop also affects ligand specificity (Parker and Boulanger, 2015). Replacing the DII loop of TgAMA1 with a shorter linker substantially enhanced the interaction between the genetically modified TgAMA1 and the heterogenous *Eimeria tenella* RON2 (EtRON2), even though TgAMA1 with an intact DII loop only interacted weakly with it (Parker and Boulanger, 2015). In the present study, the differences in DII loop sequence and length between *Eimeria* and *Plasmodium* AMA1 proteins have been given based on structural prediction of EtAMA1, providing preliminary information for future investigations into how possible divergences may influence the functional biology of EtAMA1.

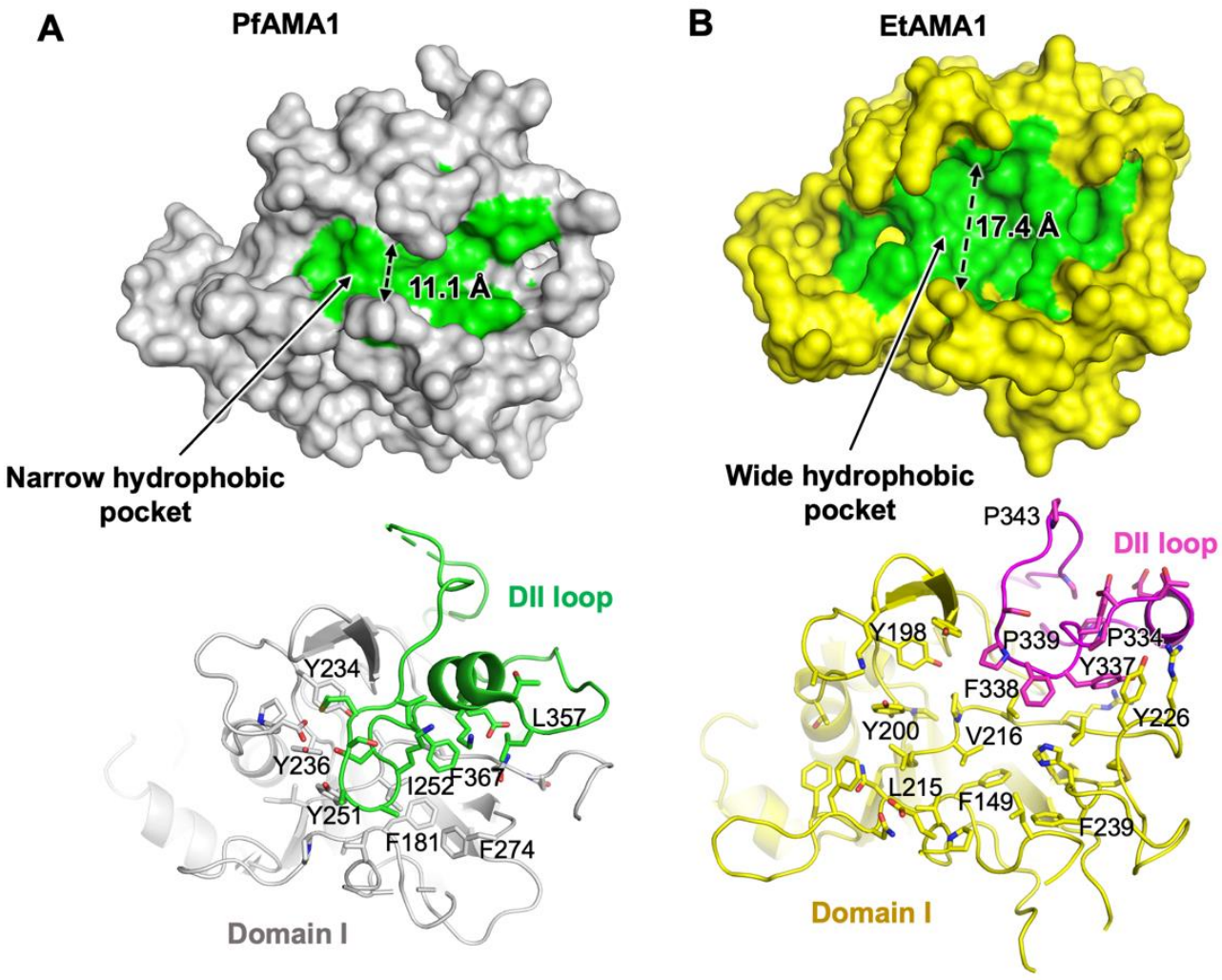

Figure 4. The hydrophobic pocket of apical membrane antigen 1 (AMA1) proteins. **A:** Crystal structure of the *Plasmodium falciparum* AMA1 (PfAMA1), shown in surface representation with the hydrophobic pocket highlighted in green (upper panel), and in cartoon representation with the loop of domain II (DII loop) colored in green (lower panel). **B:** AlphaFold-predicted structure of *Eimeria tenella* AMA1 (EtAMA1), shown in surface representation with the hydrophobic pocket highlighted in green (upper panel), and in cartoon representation with the loop of domain II (DII loop) colored in pink (lower panel). Residues at the hydrophobic pocket are indicated. The two-headed dashed arrows indicate the widths of the hydrophobic pocket, as estimated in angstroms using PyMOL.

Structural characteristics of domain III in *Eimeria tenella* apical membrane antigen 1

The AF3-predicted structure of EtAMA1 possesses a DIII, characterized by three antiparallel β-strands, forming a β-pleated sheet (Figure 5A). Structural elements of DIII in EtAMA1 were also predicted for *Eimeria maxima* AMA1 (EmAMA1; Figure 5B). Sequence alignment confirmed that five of six cysteine residues in DIII are strictly conserved

across *Eimeria*, suggesting that disulfide linkages may be conserved among *Eimeria* species. The NMR structure of DIII from PfAMA1 (PDB ID: 1HN6; Nair et al., 2002) and the crystal structure of DIII from *Plasmodium vivax* AMA1 (PvAMA1; PDB ID: 1W8K; Pizarro et al., 2005) have been previously reported; thus, they are used in the present study for comparative analysis of DIII (Figure 5C and 5D). The DIII structure of PvAMA1 contains a great number of structural elements, beginning with an N-terminal α-helix followed by an unstructured loop, then a β-strand, and a short α-helix packed against a small three-stranded β-sheet, and finally a β-hairpin positioned alongside another α-helix (Figure 5C). On the other hand, DIII of PfAMA1 features a short α-helix preceded by 50-residue-long disordered loop and a short β-hairpin (Figure 5D). The overall topology of the predicted DIII structure of EtAMA1 does not resemble any of the two *Plasmodium* DIII structures, while the local substructure displays certain similarity. In particular, while each *Plasmodium* DIII structure contains an α-helix followed by an extended disordered loop in the N-terminal region of DIII, EtAMA1 lacks all of these. Nevertheless, two β-strands of the three-stranded β-sheet in DIII of EtAMA1 (residues 414-431 in EtAMA1) can be superimposed with the β-hairpin of DIII in PfAMA1 (residues 492-509 in PfAMA1), with an RMSD between Cα atoms of 1.1 Å. Three disulfide bonds (C397-C420, C408-C432, and C413-C440) are present in the DIII model of EtAMA1 (Figure 5A). While the same number of disulfide bonds is present in the *Plasmodium* DIII structures, the sequence alignment revealed that only one out of six Cysteines is invariant in EtAMA1 (corresponding to C408 in EtAMA1; Figure 1). In summary, the structural topology of DIII in EtAMA1 is speculated to differ markedly from that of PvAMA1 and PfAMA1. Notwithstanding, experimental determination of its structure will be necessary to validate these predictions and to reveal the functional implications of possible divergence.

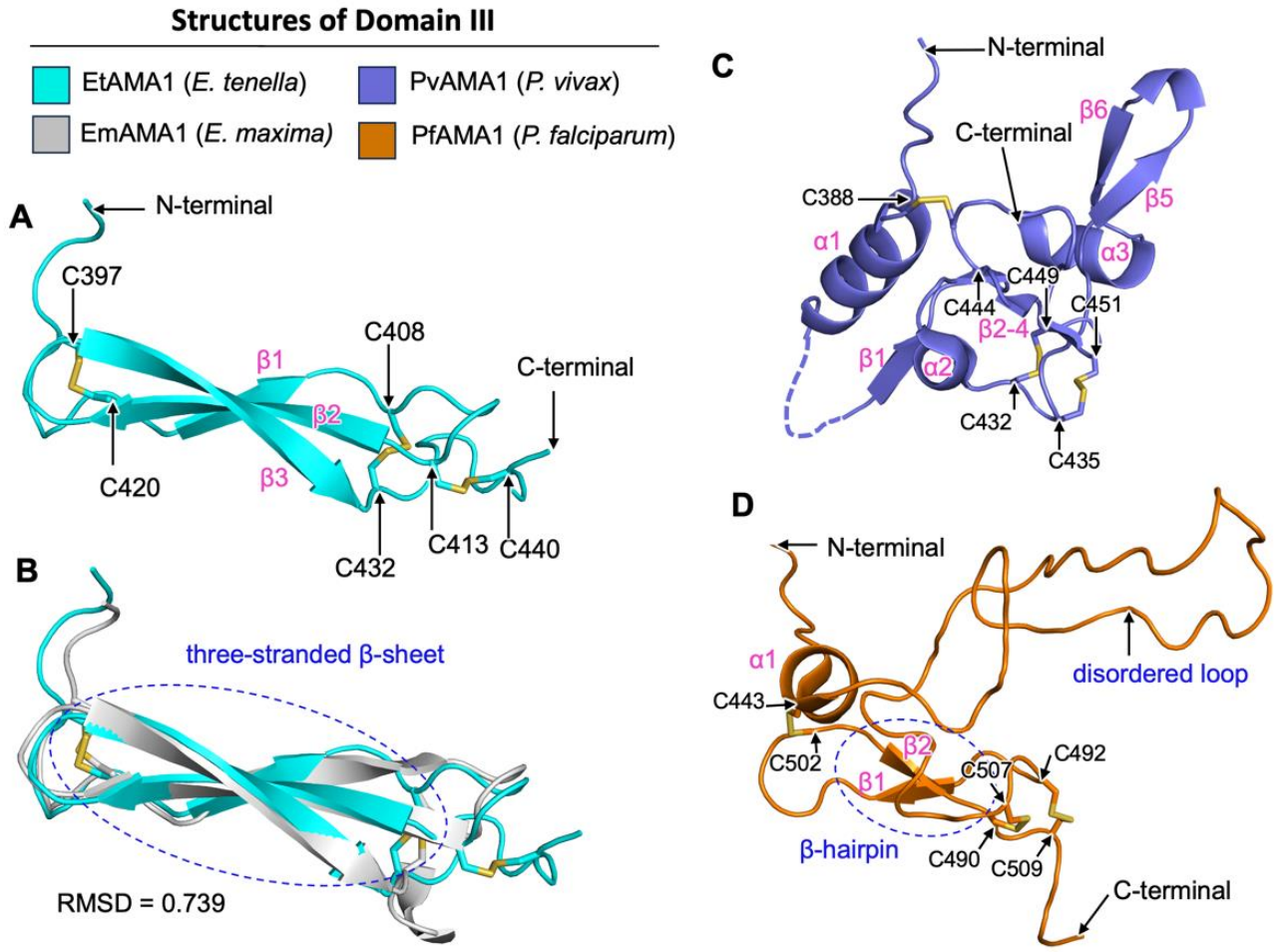

Figure 5. Domain III of apical membrane antigen 1 (AMA1) proteins. The secondary structure elements of domain III are annotated according to standard conventions, with α-helices labeled sequentially as α1, α2, α3, and β-strands labeled sequentially as β1, β2, β3 to β6 following their order along the polypeptide chain. **A:** The predicted domain III structure of *Eimeria tenella* AMA1 **(**EtAMA1) features a three-stranded β-sheet (β1-β3). **B:** Structural superposition of predicted domain III models from EtAMA1 and *Eimeria maxima* AMA1 **(**EmAMA1). The root mean square deviation between the Cα atoms of the two structures is 0.739Å. **C:** The crystal structure of domain III of *Plasmodium vivax* AMA**1** (PvAMA1) features an N-terminal α-helix (α1) followed by an unstructured loop, then a β-strand (β1), and a short α-helix (α2) packed against a small three-stranded β-sheet (β2-β4), and finally a β-hairpin (β5-β6) positioned alongside another α-helix (α3). **D:** The NMR structure of domain III of *Plasmodium falciparum* AMA**1** (PfAMA1) possesses an N-terminal α-helix (α1) followed by a long disordered loop and finally a β-hairpin (β1-β2). Cysteine residues that formed disulfide bonds in domain III are indicated.

CONCLUSION

The present study presents a sequence alignment and a comparative structural analysis of *Eimeria tenella* apical membrane antigen 1 (EtAMA1) based on AlphaFold3 prediction. Although overall sequence identity between EtAMA1 and *Plasmodium falciparum* AMA1 (PfAMA1) is low (19%), the core architecture of domains I and II, including the PAN motif and the disulfide framework, may be preserved. While five aromatic residues forming the hydrophobic pocket for ligand binding in PfAMA1 are conserved in EtAMA1, the substitutions of Y251 and I252 in PfAMA1 with L215 and V216 in EtAMA1 suggest that specific interactions with ligand may differ. The shorter, proline-rich DII loop of EtAMA1 could cover less of the hydrophobic pocket, a difference that could be functionally relevant, although this remains to be experimentally verified. Domain III of EtAMA1 is also predicted to diverge significantly in topology from *Plasmodium* DIII structures, with a three-stranded β-sheet stabilized by three disulfide bonds. Overall, the present study predicted regions of conservation shared between *Plasmodium* and *Eimeria*, as well as potential *Eimeria*-specific structural divergences, based on AlphaFold3. Structural insights into the *Eimeria*-specific hydrophobic pocket and domain III may inform the design of binding peptides to *Eimeria* AMA1 capable of inhibiting host cell invasion, a strategy that has been established in malaria disease. As the interpretations rely on AlphaFold3 prediction, future experimental determination of EtAMA1 structure and ligand-binding characteristics will be essential to validate the results and to clarify their biological significance.

DECLARTIONS

Acknowledgements

The authors would like to thank Hue University for partial support of this study under the Core Research Program.

Author contributions

All authors contributed to the study conception and design. Material preparation, data collection, and analysis were performed by Pham Hoang Son Hung, Ho Thi Dung, Duong Thanh Hai, and Tran Nguyen Thao. The first draft of the manuscript was written by Pham Hoang Son Hung, and all authors commented on previous versions of the manuscript. All authors read and approved the final edition of the manuscript.

Availability of data and materials

Protein sequences and crystal structures used for analysis in this study are provided in the manuscript.

Competing interests

The authors declare that they have no competing interests. The corresponding author takes full responsibility for any conflicts of interest or published content.

Ethical considerations

The authors declare that they did not use artificial intelligence (AI) for the designing the study, writing the manuscript, nor for the creation of images, graphics, tables, or captions. Also authors confirmed that the manuscript was checked for plagiarism and no duplicate publication was done.

Funding

The present study received no funding or financial support.

REFERENCES

Abramson J, Adler J, Dunger J, Evans R, Green T, Pritzel A, Ronneberger O, Willmore L, Ballard AJ, Bambrick J et al. (2024). Accurate structure prediction of biomolecular interactions with AlphaFold 3. Nature, 630(7943): 493-500. DOI: https://www.doi.org/10.1038/s41586-024-07487-w

Bai T, Becker M, Gupta A, Strike P, Murphy VJ, Anders RF, and Batchelor AH (2005). Structure of AMA1 from *Plasmodium falciparum* reveals a clustering of polymorphisms that surround a conserved hydrophobic pocket. Proceedings of the National Academy of Sciences of the United States of America, 102(36): 12736-12741. DOI: https://www.doi.org/10.1073/pnas.0501808102

Besteiro S, Dubremetz JF, and Lebrun M (2011). The moving junction of apicomplexan parasites: A key structure for invasion. Cellular Microbiology, 13(6): 797-805. DOI: https://www.doi.org/10.1111/j.1462-5822.2011.01597.x

Besteiro S, Michelin A, Poncet J, Dubremetz JF, and Lebrun M (2009). Export of a *Toxoplasma gondii* rhoptry neck protein complex at the host cell membrane to form the moving junction during invasion. PLoS Pathogens, 5(2): e1000309. DOI: https://www.doi.org/10.1371/journal.ppat.1000309

Blake DP, Knox J, Dehaeck B, Huntington B, Rathinam T, Ravipati V, Ayoade S, Gilbert W, Adebambo AO, Jatau ID et al. (2020). Re-calculating the cost of coccidiosis in chickens. Veterinary Research, 51(1): 115. DOI: https://www.doi.org/10.1186/s13567-020-00837-2

Chuang I, Sedegah M, Cicatelli S, Spring M, Polhemus M, Tamminga C, Patterson N, Guerrero M, Bennett JW, McGrath S et al. (2013). DNA prime/adenovirus boost malaria vaccine encoding *P. falciparum* CSP and AMA1 induces sterile protection associated with cell-mediated immunity. PLoS ONE, 8(2): e55571. DOI: https://www.doi.org/10.1371/journal.pone.0055571

Crawford J, Tonkin ML, Grujic O, and Boulanger MJ (2010). Structural characterization of apical membrane antigen 1 (AMA1) from *Toxoplasma gondii*. Journal of Biological Chemistry, 285(20): 15644-15652. DOI: https://www.doi.org/10.1074/jbc.M109.092619

Delgadillo RF, Parker ML, Lebrun M, Boulanger MJ, and Douguet D (2016). Stability of the *Plasmodium falciparum* AMA1-RON2 complex is governed by the domain II (DII) loop. PLoS One, 11(1): e0144764. DOI: https://www.doi.org/10.1371/journal.pone.0144764

Fukutani T, Miyazawa K, Iwata S, and Satoh H (2021). G-RMSD: Root mean square deviation based method for three-dimensional molecular similarity determination. Bulletin of the Chemical Society of Japan, 94(2): 655-665. DOI: https://www.doi.org/10.1246/bcsj.20200258

Guo HB, Perminov A, Bekele S, Kedziora G, Farajollahi S, Varaljay V, Hinkle K, Molinero V, Meister K, Hung C et al. (2022). AlphaFold2 models indicate that protein sequence determines both structure and dynamics. Scientific Report, 12: 10696. DOI: https://www.doi.org/10.1038/s41598-022-14382-9

Harvey KL, Yap A, Gilson PR, Cowman AF, and Crabb BS (2014). Insights and controversies into the role of the key apicomplexan invasion ligand, apical membrane antigen 1. International Journal for Parasitology, 44(12): 853-857. DOI: https://www.doi.org/10.1016/j.ijpara.2014.08.001

Jumper J, Evans R, Pritzel A, Green T, Figurnov M, Ronneberger O, Tunyasuvunakool K, Bates R, Zidek A, Potapenko A et al. (2021). Highly accurate protein structure prediction with AlphaFold. Nature, 596(7873): 583-589. DOI: https://www.doi.org/10.1038/s41586-021-03819-2

Kovalevskiy O, Mateos-Garcia J, and Tunyasuvunakool K (2024). AlphaFold two years on: Validation and impact. Proceedings of the National Academy of Sciences of the United States of America, 121(34): e2315002121. DOI: https://www.doi.org/10.1073/pnas.2315002121

Lamarque M, Besteiro S, Papoin J, Roques M, Vulliez-Le Normand B, Morlon-Guyot J, Dubremetz JF, Fauquenoy S, Tomavo S, Faber BW et al. (2011). The RON2-AMA1 interaction is a critical step in moving junction-dependent invasion by apicomplexan parasites. PLoS Pathogens, 7(2): e1001276. DOI: https://www.doi.org/10.1371/journal.ppat.1001276

Li J, Wang F, Ma C, Huang Y, Wang D, and Ma D (2018). Recombinant *Lactococcus lactis* expressing *Eimeria tenella* AMA1 protein and its immunological effects against homologous challenge. Experimental Parasitology, 191: 1-8. DOI: https://www.doi.org/10.1016/j.exppara.2018.05.003

Liu Q, Jiang Y, Yang W, Liu Y, Shi C, Liu J, and Li J (2020). Protective effects of a food-grade recombinant *Lactobacillus plantarum* with surface displayed AMA1 and EtMIC2 proteins of *Eimeria tenella* in broiler chickens. Microbial Cell Factories, 19: 28. DOI: https://www.doi.org/10.1186/s12934-020-1297-4

Mariani V, Biasini M, Barbato A, and Schwede T (2013). lDDT: A local superposition-free score for comparing protein structures and models using distance difference tests. Bioinformatics, 29(21): 2722-2728. DOI: https://www.doi.org/10.1093/bioinformatics/btt473

Mathis GF, Lumpkins B, Cervantes HM, Fitz-Coy SH, Jenkins MC, Jones MK, Price KR, and Dalloul RA (2025). Coccidiosis in poultry: Disease mechanisms, control strategies, and future directions. Poultry Science, 104(5): 104663. DOI: https://www.doi.org/10.1016/j.psj.2024.104663

Nair M, Hinds MG, Coley AM, Hodder AN, Foley M, Anders RF, and Norton RS (2002). Structure of domain III of the blood-stage malaria vaccine candidate, *Plasmodium falciparum* apical membrane antigen 1 (AMA1). Journal of Molecular Biology, 322(4): 741-753. DOI: https://www.doi.org/10.1016/s0022-2836(02)00806-9

Ouattara A, Takala-Harrison S, Thera MA, Coulibaly D, Niangaly A, Saye R, Tolo Y, Dutta S, Heppner DG, Soisson L et al. (2013). Molecular basis of allele-specific efficacy of a blood-stage malaria vaccine: vaccine development implications. The Journal of Infectious Diseases, 207(3): 511-519. DOI: https://www.doi.org/10.1093/infdis/jis709

Parker ML and Boulanger MJ (2015). An extended surface loop on Toxoplasma gondii apical membrane antigen 1 (AMA1) governs ligand binding selectivity. PLoS ONE, 10(5): e0126206. DOI: https://www.doi.org/10.1371/journal.pone.0126206

Pastor-Fernandez I, Kim S, Billington K, Bumstead J, Marugan-Hernández V, Küster T, Ferguson DJP, Vervelde L, Blake DP, and Tomley FM (2018). Development of cross-protective *Eimeria*-vectored vaccines based on apical membrane antigens. International Journal for Parasitology, 48(7): 505-518. DOI: https://www.doi.org/10.1016/j.ijpara.2018.01.003

Pham HHS, Matsubayashi M, Tsuji N, and Hatabu T (2021). Relationship between *Eimeria tenella* associated-early clinical signs and molecular changes in the intestinal barrier function. Veterinary Immunology and Immunopathology, 240: 110321. DOI: https://www.doi.org/10.1016/j.vetimm.2021.110321

Pizarro JC, Vulliez-Le Normand B, Chesne-Seck ML, Collins CR, Withers-Martinez C, Hackett F, Blackman MJ, Faber BW, Remarque EJ, Kocken CH et al. (2005). Crystal structure of the malaria vaccine candidate apical membrane antigen 1. Science, 308(5720): 408-411. DOI: https://www.doi.org/10.1126/science.1107449

Quiroz-Castaneda RE (2018). Avian coccidiosis, new strategies of treatment. avian coccidiosis, new strategies of treatment. Farm animals diseases, recent omic trends and new strategies of treatment. InTech., United Kingdom, pp. 119-133. DOI: https://www.doi.org/10.5772/intechopen.74008

Robert X and Gouet P (2014). Deciphering key features in protein structures with the new ENDscript server. Nucleic Acids Research, 42(W1): W320-W324. DOI: https://www.doi.org/10.1093/nar/gku316

Srinivasan P, Beatty WL, Diouf A, Herrera R, Ambroggio X, Moch JK, Tyler JS, Narum DL, Pierce SK, Boothroyd JC et al. (2011). Binding of *Plasmodium* merozoite proteins RON2 and AMA1 triggers commitment to invasion. Proceedings of the National Academy of Sciences, 108(32): 13275-13280. DOI: https://www.doi.org/10.1073/pnas.1110303108

Tonkin ML, Roques M, Lamarque MH, Pugniere M, Douguet D, Crawford J, Lebrun M, and Boulanger MJ (2011). Host cell invasion by apicomplexan parasites: Insights from the co-structure of AMA1 with a RON2 peptide. Science, 333(6041): 463-467. DOI: https://www.doi.org/10.1126/science.1204988

Tyler JS, Treeck M, and Boothroyd JC (2011). Focus on the ringleader: the role of AMA1 in apicomplexan invasion and replication. Trends in Parasitology, 27(9): 410-420. DOI: https://www.doi.org/10.1016/j.pt.2011.04.002

Vulliez-Le Normand B, Tonkin ML, Lamarque MH, Langer S, Hoos S, Roques M, Saul FA, Faber BW, Bentley GA, Boulanger MJ et al. (2012). Structural and functional insights into the malaria parasite moving junction complex. PLoS Pathogen, 8(6): e1002755. DOI: https://www.doi.org/10.1371/journal.ppat.1002755

Wang G, Drinkwater N, Drew DR, MacRaild CA, Chalmers DK, Mohanty B, Lim SS, Anders RF, Beeson JG, Thompson PE et al. (2016). Structure–activity studies of β-hairpin peptide inhibitors of the *Plasmodium falciparum* AMA1–RON2 interaction. Journal of Molecular Biology, 428(20): 3986-3998. DOI: https://www.doi.org/10.1016/j.jmb.2016.07.001

Wang Q, Zhao Q, Zhu S, Huang B, Yu S, Liang S, Wang H, Zhao H, Han H, and Dong H (2020). Further investigation of the characteristics and biological function of *Eimeria tenella* apical membrane antigen 1. Parasite, 27: 70. DOI: https://www.doi.org/10.1051/parasite/2020068